NASA Technical Memorandum 81784

NASA-TM-81784 19800012045

Complete Supersonic Flowfields Over Blunt Bodies in a Generalized Orthogonal Coordinate System

Peter A. Gnoffo

March 1980

National Aeronautics and Space Administration

Langley Research Center
Hampton, Virginia 23665

Complete Supersonic Flowfields Over Blunt Bodies In a Generalized Orthogonal Coordinate System

Peter A. Gnoffo*
NASA Langley Research Center
Hampton, Virginia

Abstract

A general orthogonal coordinate system is used to describe various axisymmetric and two-dimensional shapes. Close approximations to planetary probe configurations are possible. The full Navier-Stokes equations are discretized in this coordinate system in a manner based on Allen and Cheng's numerical procedure. The bow shock is treated as a discontinuity which floats between grid points. Completely coupled flows over the forebody, base, and near wake have been calculated over a cylinder, sphere, and an approximation to the Viking Aeroshell for $2 \leq M_\infty \leq 10$ and $1000 \leq Re \leq 30{,}000$. The program gives good comparisons with experimental data. A major contribution of this work is that it allows one to study the effect of changes in the blunt body shape on the base flow structure. Also, some problem areas in determining the base flow for increasing Reynolds number are discussed. In particular, it is found that the mean free path of the fluid near the wall immediately below the corner of the Viking Aeroshell, which experiences a severe expansion, can become greater than the local mesh size required to resolve the boundary layer in the forebody. Negative pressures, densities, and temperatures can be calculated in these instances. It appears that part of this problem is due to an inability to capture a lip shock close to the wall with the given grid.

---

*Aero-Space Technologist, Aerothermodynamics Branch, Space Systems Division. Presently involved in Graduate Study at Princeton University, Princeton, New Jersey.

Nomenclature

A_n, B, C	transformations constants, nondimensionalized by R_N
a	speed of sound, m/sec
a_{1-4}	coordinate stretching constants used in Eq. (3)
B_s, R_s, C	shock shape parameters in Eq. (6)
f_1, f_2	functions defined in Eq. (3)
H	total enthalpy nondimensionalized by V^2_∞
h	metric coefficient, nondimensionalized by R_N
i,j	indices on node points (Fig. 2)
k	heat transfer coefficient, $W/m\text{-}^oK$
L	length of recirculation region along axis, nondimensionalized by R_N
M	Mach number
NI	total number of node points in θ direction
NJ	total number of node points in η direction
n	direction normal to wall, m
Pr	Prandtl number
p	pressure nondimensionalized by $\rho_\infty V^2_\infty$
q	heat transfer, W/m^2
Re	Reynolds number - based on nose radius of curvature
R_N	nose radius of curvature, m
T	temperature, nondimensionalized by T_∞
T_∞	freestream temperature, ^oK
T_o	stagnation temperature, ^oK
t	time nondimensionalized by R_N/V_∞

u,v	velocities directed along lines of constant r and θ respectively, nondimensionalized by V_∞
V_∞	freestream velocity, m/sec
x,y,z	Cartesian coordinates, nondimensionalized by R_N
Y	metric, nondimensionalized by R_N = 1 (2D case) = distance from axis in axisymmetric case
γ	ratio of specific heats
δ	shock standoff distance, normal to body nondimensionalized by R_N
δ_o	initial guess on shock standoff distance on an axis, nondimensionalized by R_N
ε	smoothing constant in Eq. (5)
η	transformed r coordinate
θ,r,ϕ	transformed coordinates
θ_{sep}	value of θ where flow separates in the base
μ	viscosity, nondimensionalized by $\mu(T_\infty)$
ν	Mach angle
ρ	density nondimensionalized by ρ_∞
ρ_∞	freestream density, kg/m^3
ψ	angle defined by Eq. (7) and Fig. 3

Subscripts:

w	wall
∞	freestream

Introduction

Currently projected missions to probe the atmospheres of the outer planets have raised questions concerning the influence of base flow on the low density aerodynamics of a probe and the radiative heating levels imposed on a probe afterbody. The radiative heating levels on the forebody will be severe and although the ratio of afterbody to forebody heating is expected to be small the magnitude of the afterbody heating can still be significant. A lip shock standing off the body just upstream of the separation point adds to the complexity of the base flow, and makes it difficult to solve the base flow problem on a computer.

There are two general approaches for attacking this problem computationally: 1) The coupling of several approximate techniques which are designed to model specific features of the flowfield, the so called "patchwork" approach, and 2) the solution of the full Navier-Stokes equations in the entire flowfield.[1,2,3,4] Both of these approaches have their own advantages and disadvantages. Several approximate techniques for the solution of wake flows have been presented in the literature[5,6,7,8,9] and summaries of these results are available.[10,11,12] Solutions to the Navier-Stokes equations in the base region using specified conditions on the inflow boundary have also been presented in the literature.[13,14] In general, these approximate techniques offer the advantage of obtaining solutions rapidly on the computer. However, the nature of the various approximations can distort the results and usually these techniques are restricted to specific body

geometries and flow regimes. A solution of the full Navier-Stokes equations in the entire flowfield eliminates the need for making the various assumptions required for the approximate solutions. However, solutions of the Navier-Stokes equations typically require a great deal of computational time and storage. Ideally, one should be able to use the two solution approaches to complement each other; i.e., use the Navier-Stokes solutions to improve the nature of the approximations in the approximate techniques and use these rapidly running, specialized techniques to perform parametric studies for design analyses.

The material presented herein is a continuation of a research effort[1] which is directed toward developing a computer code which can compute full Navier-Stokes solutions around complete probe-like configurations for a wide range of supersonic Mach numbers and Reynolds numbers. As Mach number and Reynolds number are increased various flow phenomena develop (shock strengths increase; boundary layers, lip shocks, and recompression shocks form) which require special consideration within the computational code. Flowfield solutions at low supersonic Mach numbers and low Reynolds numbers were described in the previous work and good agreement was found with experimental data. Whereas the technique presented in Ref. 1 employed shock capturing throughout the flowfield, a procedure for treating the bow shock as a discontinuity which is allowed to float within the computational grid has been included in the present analysis. This capability permits the computation of higher Mach number and Reynolds number flows. An improved coordinate stretching capability has extended the Reynolds number range by making

it possible to pack more points in the boundary layer. Shock and body slip conditions have been included in the present code. Observations of flowfield characteristics and comparisons to experimental data are presented for a Mach number range $2 \leq M_\infty \leq 10$ and a Reynolds number range $1000 \leq R_e \leq 30{,}000$. In keeping with a philosophy of adding only one complicating factor at a time, only laminar, perfect gas, two-dimensional, or axisymmetric flows are considered.

It is also noted that this program is still considered in a developmental stage. Although comparisons with experimental data are encouraging there are still aspects of this approach which should be investigated more fully (these potential problem areas will be discussed in later sections). The purpose of the present paper is to report the progress of this investigation and to point out some interesting problem areas and flow phenomena that have been encountered.

Coordinate System

A generalized curvilinear orthogonal coordinate system[15] which can be used for approximating various axisymmetric and two-dimensional body shapes; including spheres, ellipses, spherically-capped cones, flat-faced cylinders with rounded corners, circular disks and planetary probes; is used herein. The transformation from the (θ, r, ϕ) domain to the (x, y, z) domain for an axisymmetric coordinate system is written as:

$$\left.\begin{aligned} x(\theta,r,\phi) &= (-B \sinh r + C \cosh r) \cos\theta - \sum_{n=2}^{N} A_n e^{nr} \cos n\theta \\ y(\theta,r,\phi) &= \left[(B \cosh r - C \sinh r) \sin\theta + \sum_{n=2}^{N} A_n e^{nr} \sin n\theta\right]\cos\phi \\ z(\theta,r,\phi) &= \left[(B \cosh r - C \sin r) \sin\theta + \sum_{n=2}^{N} A_n e^{nr} \sin n\theta\right]\sin\phi \end{aligned}\right\} \quad (1)$$

where N is a positive integer greater than two and A_n, B, and C are arbitrary constants. A two-dimensional transformation to the x,y plane is obtained by setting $\phi = 0$. Lines of constant r are transformed to circles in the x,y plane as r increases without limit through negative values. The line $r = 0$ forms the body in the x,y plane. The outflow boundary of the computational space is mapped to infinity (i.e. a circle of infinite radius) using an additional transformation. An example of a body with the associated coordinate system is shown in Fig. 1. The metric coefficients h_θ and h_r are equal in this coordinate system, thus saving considerable computational time and storage.

Analytic Development

The Navier-Stokes equations written in an orthogonal curvilinear coordinate system may be obtained from the literature.[16] Since only the steady-state solution is desired, a term involving the temporal derivative of pressure has been omitted from the energy equation in order to simplify the numerical procedure. The convective terms in the governing equations are written in conservation form as recommended[17] for shock capturing whereas the dissipative terms are expanded in terms of u, v, H, and μ. (Even though the bow shock is fitted it is assumed that we will be able to capture the lip shock and recompression shock in the base.)

In preliminary numerical calculations it was found that finite-difference approximations of terms involving products of metric coefficients with the conservative flow variables (i.e. $\partial(h\rho u)/\partial\theta$, $\partial[h^2(p+\rho u^2)]/\partial\theta$ etc.) caused large errors in the numerical solution at large distances from the body where coordinate stretching was significant. Writing the governing equations in a form which separated derivatives of metric coefficients, which are evaluated analytically, from derivatives of conservation flow variables, which are evaluated numerically, eliminated this problem. The governing equations expanded in this manner become:

$$\partial\rho/\partial t = -[\partial\rho u/\partial\theta + \partial\rho v/\partial r + \rho u(1/Y\ \partial Y/\partial\theta + 1/h\ \partial h/\partial\theta)$$

$$+ \rho v(1/Y\ \partial Y/\partial r + 1/h\ \partial h/\partial r]/h \qquad a$$

$$\partial\rho u/\partial t = -[\partial(p + \rho u^2)/\partial\theta + \partial\rho uv/\partial r - \rho v^2\ 1/h\ \partial h/\partial\theta$$

$$+ \rho u^2(1/Y\ \partial Y/\partial\theta + 1/h\ \partial h/\partial\theta) + \rho uv(1/Y\ \partial Y/\partial r + 2/h\ \partial h/\partial r)]/h$$

$$+ F_1/(h^2R_e) \qquad b$$

$$\partial\rho v/\partial t = -[\partial\rho uv/\partial\theta + \partial(p + \rho v^2)/\partial r - \rho u^2\ 1/h\ \partial h/\partial r$$

$$+ \rho v^2(1/Y\ \partial Y/\partial r + 1/h\ \partial h/\partial r) + \rho uv(1/Y\ \partial Y/\partial\theta + 2/h\ \partial h/\partial\theta)]/h \qquad (2)$$

$$+ F_2/(h^2R_e) \qquad c$$

$$\partial\rho H/\partial t = -[\partial\rho uH/\partial\theta + \partial\rho vH/\partial r + \rho uH(1/Y\ \partial Y/\partial\theta + 1/h\ \partial h/\partial\theta)$$

$$+ \rho vH(1/Y\ \partial Y/\partial r + 1/h\ \partial h/\partial r)]/h$$

$$+ F_3/(h^2R_e) + F_4/(h^2R_eP_r) \qquad d$$

where F_{1-4} are various dissipation functions defined in Ref. 1 with $\mu = \mu(T)$ using Sutherland's law and Pr = constant.

An additional coordinate transformation is utilized which simplifies the treatment of the outflow boundary by mapping it to infinity where

conditions are known and gives some control in the density of mesh points near the body. The new coordinate η is defined so that

$$r = -\ell n(f_1)/f_2 \qquad a$$

$$f_1 = 1 + a_1(1 - \eta) \qquad b \quad (3)$$

$$f_2 = a_2\eta^{a_3} + a_4\eta \qquad c$$

This stretching does not affect the orthogonality of coordinate system. Derivatives with respect to r are rewritten as derivatives with respect to η as follows:

$$\partial f/\partial r = \partial f/\partial \eta \; \partial \eta/\partial r$$

$$\partial^2 f/\partial r^2 = \partial^2 f/\partial \eta^2 (\partial \eta/\partial r)^2 + \partial f/\partial \eta \; \partial^2 \eta/\partial r^2$$

where $\partial \eta/\partial r$ and $\partial^2 \eta/\partial r^2$ can be obtained algebraically.

Numerical Approach

All of the material presented in this section, except for the discussion on shock floating and initial conditions, is described in Ref. 1. For the sake of brevity and completeness, only a brief summary of material presented in the earlier work is presented.

A modification of the Brailovskaya scheme which was introduced by Allen and Cheng[13,18] was applied to the governing equations. This particular method was chosen because the viscous stability limit in the numerical procedure is removed. The stability limit on the time step for the inviscid terms is written as

$$\Delta t \leq 1/[|u|/(h\Delta\theta) + |v|/(h\,\partial r/\partial\eta\,\Delta\eta) + a\sqrt{1/(\Delta\theta^2) + 1/(\partial r/\partial r_i\,\Delta\eta)^2}/h] \tag{4}$$

where a is the local speed of sound.

Preliminary calculations indicated that a smoothing routine was necessary to eliminate numerical instabilities which occur in the vicinity of a captured shock and in the wake. A nonphysical damping function was used to eliminate these instabilities.[19] Terms of fourth order in the spatial grid are used to smooth the variables ρ, ρu, ρv, and ρH after every iteration. For example

$$\rho_{i,j}^{n+1} = \tilde{\rho}_{i,j}^{n+1} - \varepsilon[(\Delta\theta)^4\partial^4\rho/\partial\theta^4 + (\Delta\eta)^4\,\partial^4\rho/\partial\eta^4]_{i,j}^{n} \tag{5}$$

The tilde indicates the undamped results from the corrector step of the difference scheme and ε is a constant such that $0 \leq \varepsilon \leq 1/24$. Small variations to the smoothing formulas must be implemented near the boundaries $j = 1$, $j = NJ$ and in the vicinity of the fitted bow shock (Fig. 2).

Initial Conditions - The initial shock shape is prescribed by the formula (similar to one by Van Dyke[20])

$$y_s^2 = 2R_s x_1^c - B_s x_1^2 \tag{6}$$

where

$$B_s = 1/(1-M_\infty^2) \quad , \quad 0 < c < 2, \; R_s > 0$$

$$x_1 = x - x_0, \text{ and } \quad x_0 = \delta_0 + x(\pi,0)$$

(The constant $c = 1$ yields an hyperbola, $c \to 0$ causes the Mach angle, ν, to be approached more quickly, and R_s controls the magnitude of y_s at a particular x location). The points of intersection (values of r) where lines of constant θ intersect the shock are determined implicitly. The shock angle is calculated and conditions on the shock at these points are evaluated using the Rankine-Hugoniot equations. The no-slip conditions are imposed on the body. A stagnation pressure is calculated and the pressure distribution around the body is assumed to vary as the cosine squared of the body angle, until the freestream pressure is achieved, at which point the pressure on the body is held at p_∞. An isentropic expansion around the body is used to approximate

the distribution of ρ and H. The quantities p, ρ, u, and v are assumed to vary linearly in η between the shock and the body along lines of constant θ, and H is calculated from the equation of state. A linear variation of these quantities in η based on freestream values of p, ρ, u, and v is used in the base region where lines of constant θ do not intersect the shock.

The components of the uniform freestream velocity field in the present coordinate system are calculated as $v = -\sin\psi$ and $u = \cos\psi$, where ψ is the angle of the vector tangent to a line of constant r in a direction of increasing θ, measured in a counterclockwise direction from the horizontal (Fig. 3). The differentials dx and dy along a line of constant r can be determined from Eq. (1) and may be used to show that

$$\left.\begin{aligned} \cos\psi &= \frac{(B\sinh r - C\cosh r)\sin\theta + \sum_{n=2}^{N} nA_n e^{nr}\sin n\theta}{h} \quad \text{a} \\ \sin\psi &= \frac{(B\cosh r - C\sinh r)\cos\theta + \sum_{n=2}^{N} nA_n e^{nr}\cos n\theta}{h} \quad \text{b} \end{aligned}\right\} \tag{7}$$

Shock Floating - The shock floating technique, treating the shock as a discontinuity which lies between mesh points in the computational field (Fig. 2), has been described by Moretti,[21,22] Salas,[23] and Daywitt, et al.[24] Treating the bow shock as a discontinuity using the Rankine-Hugoniot equations eliminates the problem, associated with shock capturing, of creating a numerical overshoot and undershoot of properties near the shock, possibly causing static enthalpy to go negative. The choice of shock floating over nondimensionalizing by shock displacement

was made for two reasons. Shock displacement along a line of constant θ becomes unbounded in the base region; and, for small values of θ near the base symmetry plane, lines of constant θ never intersect the shock. Also, nondimensionalizing by shock displacement destroys the orthogonality of the coordinate system and consequently further complicates the governing equations.

The shock position is tracked along lines of constant θ. This coordinate is the obvious choice in the stagnation region because lines of constant θ are nearly normal to the bow shock here. However, in sweeping around the body in a clockwise direction, it is found that these lines intersect the shock at smaller angles; consequently, a small displacement of shock position in a direction normal to the shock (which is the direction shock velocities are determined) is seen as a large displacement along a line of constant θ. The shock position could be tracked along lines of constant η in these situations; however, the bookkeeping and internal logic would become more complex. It has been found that lines of constant θ can be used to track the shock movement so long as one ensures that the shock angle never becomes less than the Mach angle during the iteration process.

The shock floating algorithm cannot be described in detail here because of space limitations but a general description is supplied below. The numerical procedure at interior points is described in Ref. 1. Special difference formulas are used when the shock cuts a computational molecule. A predictor step is performed at mesh points behind and on the bow shock. Pressure behind the shock and the shock angle determines shock velocity. These velocities are resolved along coordinate directions to

obtain shock displacement. The Rankine-Hugoniot equations for a moving shock are used to redefine ρ, u, v, and H on the shock. The procedure is repeated for the corrector step. Some damping of the shock motion and smoothing of the shock shape are necessary early in the iteration process; however, these fixes can be turned off when the shock approaches a steady position. The shock converges rapidly in the stagnation region and more slowly downstream where the shock angle approaches the Mach angle. Depending on the severity of the "misalignment" of the initial shock shape, a wave in the shock can be observed to travel downstream. The use of central differences to calculate shock angle in the forebody region, where the flow behind the shock is subsonic or transonic, and forward differences downstream, prevented these waves from reflecting back into the stagnation region, thus speeding convergence. Sometimes this wave caused the shock angle to become less than the Mach angle. In such situations, rather than use the Rankine-Hugoniot equations which are invalid, shock displacement is defined in a manner to force the shock angle to equal the Mach angle.

Results and Discussion

All of the material presented herein, unless otherwise noted, was computed on a grid of 51 x 50, with $a_1 = 1.5$, $a_2 = 1$, $a_3 = 2$, and $a_4 = 1.5$. The constants describing the cylinder are $B = C = 1$, $A_n = 0$. The constants describing the Viking Aeroshell (Fig. 1) are $B = 1.5146477$, $C = 0.71607873$, $A_2 = -0.059786238$, $A_3 = -0.056648540$, and $A_4 = 0.042817883$.

General Observations - For the given initial conditions, a region of high density and pressure builds up in the base area and eventually flows out toward the outflow boundary. The formation of this high density region produces gradients which can cause instabilities in the wake. These instabilities can be controlled by adjusting the value of the smoothing parameter, ε, and by decreasing the integration time step to some fraction, ($\approx 1/10$) of the stability limit of Eq. (4). At times, it is necessary to iterate only in the base flow region, while holding the rest of the field constant. These problems become more severe as M_∞ and Re_∞ are increased. Many of these problems can be alleviated by starting the procedure with a low Reynolds number for the first few thousand iterations. It is advisable to iterate the solution during this period in blocks of 500 iterations in order to ascertain the effect of changes in the smoothing parameter, the time step, or the Reynolds number, always picking up in the new solution where the old solution left off. When one has passed the hurdle of integrating in time beyond these artificially induced transients and instabilities the time step can be raised to the full stability limit and ε can be decreased.

Note that many of these problems could be overcome by establishing more realistic initial conditions in this coordinate system. Also, it is possible that a given set of initial conditions may result in transients that are too complex to be resolved by the present technique. This is especially true for the initial guess on shock shape at high Mach numbers. The smoothing that was incorporated into the program in the vicinity of the shock is designed to allow the solution to progress from a relatively large error in the initial shock shape. Still, it is possible to specify an initial shock shape that cannot be iterated to convergence. In such cases it is useful to study the history of the shock motion (i.e., Is the shock moving in or out? Is the shock bluntness in the nose region increasing or decreasing?) and adjust the parameters of the initial shock shape (Eq. (6)) accordingly. It should also be noted that the fix of using a low Reynolds number initially, as mentioned in the previous paragraph, can sometimes make the shock floating process more difficult (i.e., there really is no discrete shock to track). In such cases some compromise must be found in choosing the values of Re and ε to be used. Experience dictates the best choice and is the best teacher in these situations.

Convergence is achieved within 15,000 iterations. It is defined by looking at the value $E = |(\rho^{n+1} - \rho^n)/\rho^n|$ and at the distribution of properties along the base symmetry line. (When the maximum value of E in the field becomes less than 10^{-4} and properties on the base line of symmetry are constant to three decimal places after 1000 iterations then the solution is said to be converged.) After a converged solution

has been obtained for a particular Mach number and Reynolds number, the solution at a new Reynolds number can be obtained within approximately 5,000 iterations using the old solution as an initial condition. The same is true for changes in M_∞ that produce small changes in ν.

Some distortion of properties near the boundary $\eta = 0$ is observed. The poor resolution makes it impossible to measure vehicle drag based on an integrated momentum deficit in the wake. Mapping the outflow boundary to infinity has proved useful in these early calculations in the sense that no stability problems have ever been encountered due to this particular treatment of the boundary. However, it is believed that a more exact treatment of the outflow boundary at some finite distance downstream will make it possible to obtain better resolution of the wake throat.

Comparisons with Experimental Data: Comparisons between the present method and experimental results of Tewfic and Giedt[25] for pressure distribution and heat transfer on a cylinder are presented in Figs. 4 and 5. Shock and body slip conditions were used although the calculated effects of shock slip were negligible. Also, it appears the no-slip pressure distribution gives a better agreement to experimental data than the slip condition in the stagnation region (Fig. 4) though the effect is small. A detailed comparison of base pressure distributions agree well with experimental data for similar flow conditions. The flow separation point in Fig. 4 occurs slightly downstream of the pressure minimum, at an inflection point in the curve. The heat transfer results for the $M_\infty = 5.5$ case ($Pr = 0.77$ corresponding to 90^0 K wall temperature) agree well with the experimental data, except in the stagnation region where there is approximately an

8-percent difference (Fig. 5). The $M_\infty = 5.73$ case yield values of q which agree well with experimental data in the stagnation region, fall below experimental data for much of the forebody, and level off slightly above experimental data in the base. In both cases, the calculated heat transfer was obtained according to the formula

$$q = k\,\partial T/\partial n + \mu u\,\partial u/\partial n \qquad \text{(dimensional equation)}$$

where the second term is due to "sliding friction"[26], which accounts for slip flow effects. Possible explanations for these discrepancies include the assumptions of Pr = constant, the use of Sutherland's law at these temperatures ($T_\infty \approx 40^0$ K) and experimental error. Changes in the heat transfer results were negligible when the smoothing parameter, ε, was varied from $\varepsilon = 0.003$ to $\varepsilon = 0.0005$.

The static pressure distribution along the wake centerline of an adiabatic cylinder is compared to experimental data of McCarthy and Kubota[27] in Fig. 6. The distributions near peak centerline pressure are also plotted for the previous cases to illustrate the effect of Reynolds number. The overprediction of pressure downstream is most likely due to lack of resolution in the numerical technique. The experimental data for a laminar wake show a dip in the transverse pressure distribution across the centerline which cannot be resolved in the present computational grid. Velocity vectors around the cylinder are shown in Fig. 7. Although there is no distinct line where the

velocity vectors are sharply turned due to the presence of a recompression shock one can see the gradual turning of the vectors to a parallel direction in the vicinity of where the shock should be, even in the relatively coarse grid. (The distribution of node points can also be understood from this figure. Every other node point, in a checkerboard pattern, has a velocity vector associated with it, the arrows tail originating at the node point.) The discrepancy of base pressure is within the experimental accuracy ($\Delta p_w(\theta)/p_w(\pi) = \pm.02$).[27]

Wake centerline pressure distributions and velocity vectors are presented in Figs. 6 and 8 for a sphere at the conditions given above for $M_\infty = 5.64$. The recirculation region is seen to be slightly larger for the sphere. The maximum recirculating centerline velocity and Mach number for the sphere is greater than that of the cylinder ($v_{max} = 0.191$ for sphere, $v_{max} = 0.125$ for cylinder, $M_{max} = 0.436$ for sphere, $M_{max} = 0.288$ for cylinder). Excellent agreement for forebody pressure distribution and shock shape was obtained between the present method and the numerical method of Graves[28] (Fig. 9).

Viking Aeroshell - Calculations have been made for supersonic flow over an approximation to the Viking Aeroshell in CO_2; $\gamma = 1.285$, $Pr = 0.685$, adiabatic wall; for the following conditions: $M_\infty = 2$, $Re_\infty = 1000, 5000, 30{,}000$; $M_\infty = 5$, $Re = 5000$; $M_\infty = 10$, $Re = 1000, 5000$. Fig. 10 presents the isobars for the $M_\infty = 2$, $Re_\infty = 1000$ case. The arrows and dashed lines indicate the shift in position of the isobars for $Re_\infty = 30{,}000$. The expansion fan and the coalescence of isobars to form the recompression shock are evident in this figure. Drag coefficients and some properties of the near wake flow (separation

point, θ_{sep}, length of recirculation region, L, base pressure and temperature at $\theta = o$, $p_w(o)/p_\infty$, $T_w(o)/T_\infty$, and maximum pressure on wake centerline, p_{max}/p_∞) are presented in Table 1.

The recirculation pattern for the $M_\infty = 2$, $Re_\infty = 5000$ case is presented in Fig. 11. There are two recirculating flow patterns (clockwise rotation) separated by a small counterclockwise circulating flow. The upper recirculating region in this case seems to form a horizontal platform over which the separated flow passes. Separation occurs slightly downstream of the upper corner of the body corresponding to observations made by Hama[29] and Allen and Cheng[13] for a sharp corner body. Increasing the Mach number while holding Re_∞ constant causes the upper recirculation region to decrease in size and the separation flow angle decreases below the horizontal. At $M_\infty = 10$ this upper recirculation region vanishes. Supersonic recirculation velocities on the axis of symmetry were calculated for $M_\infty = 2$, $Re_\infty = 1000$, 5000, 30,000 and $M_\infty = 5$, $Re_\infty = 5000$. For $M_\infty = 2$, $Re_\infty = 1000$ sonic velocity was just achieved and as the Reynolds number was increased a Mach number of approximately 1.4 was attained and a small shock formed approximately 0.4 nose radii away from the base, with a radius of approximately 0.25 nose radii. The recirculation shock strengths for $M_\infty = 5$, $Re_\infty = 5000$, and $M_\infty = 2$, $Re_\infty = 1000$ are approximately equal, suggesting that such phenomena are a function of $M_\infty/\sqrt{Re_\infty}$, though clearly more calculations are needed. A calculation by Erdos and Zakkay[30] for supersonic flow over a wedge in which nearly supersonic recirculating velocity was reported is the only other mention of large recirculating velocity that was found in the literature. They conclude that the recirculation

velocity varies directly with the vorticity entering the region, up to some choking condition in the flow. The present results are consistent with that observation. Several numerical experiments in which ε and grid size were varied did nothing to change the position or strength of the shock, although changes in resolution caused some differences in pressure downstream (Fig. 12). The calculation of this "recirculation shock" is a disturbing development, even though the magnitudes of pressure and density are small in its vicinity. It has been assumed that the base flow is steady and axisymmetric, and possibly the imposition of this symmetry at the axis artificially produces the calculated phenomenon. Whatever the cause, whether it is truly physical or numerical, it is an interesting result that certainly needs more investigation before the question of its existence can be satisfactorily resolved.

A calculation was attempted for $M_\infty = 5$, $Re_\infty = 30{,}000$. This case could not be run to convergence because negative values for density, pressure, and enthalpy were calculated near the wall just below the corner of the probe. The expansion around the corner was extremely severe. Even a half cell away from the body the velocity was supersonic. Increased resolution near the body did not alter this situation. In fact, a normal mesh spacing that was just fine enough to resolve the boundary layer in the forebody was less than the mean free path immediately behind the expansion corner. No discernible boundary layer is present in this region. There is a rapid compression at the wall following the expansion, the flow becomes subsonic and then separates. This behavior may be due to the formation of a lip shock, normal to the

body, immediately below the expansion corner. This shock could not be captured with the present distribution of node points in a tangential direction and with the present formulation of the boundary conditions. The numerical undershoot of properties on the low pressure side of the shock that occurs with shock capturing would then explain the calculation of negative enthalpies. Indeed, it may be necessary to "float" the lip shock rather than smear it over several mesh points and thus destroy the detail of the flow in this region.

Concluding Remarks

Solutions of the Navier-Stokes equations for the complete flow surrounding blunt bodies in a supersonic stream can be achieved using the numerical method described herein. Good comparisons with experimental data support this statement. The given coordinate system is especially useful in that it allows one to study the differences in the wake flow structure for many realistic body shapes. For example, the Viking Aeroshell exhibited a double recirculating flow pattern, while at similar freestream conditions, a sphere exhibited only a single pattern. However, it is evident that certain areas of the wake flow will require special treatment for increasing Reynolds number (i.e., Reynolds numbers on the order of 10,000). In particular, for blunt bodies experiencing a rapid expansion around a sharp corner (i.e. Viking Aeroshell) it appears that a lip shock will need to be treated as a discontinuity. The recompression shock may also need to be treated as a discontinuity and the mesh resolution in its vicinity to be increased in order to improve calculations in the far wake (i.e., $3 \leq x \leq 100$).

References

[1]Gnoffo, Peter A., "Forebody and Afterbody Solutions of the Navier-Stokes Equations for Supersonic Flow Over Blunt Bodies in a Generalized Orthogonal Coordinate System," TP-1075, February 1978, NASA.

[2]Scala, Sinclaire M. and Gordon, Paul, "Solution of the Time-Dependent Navier-Stokes Equations for the Flow Around a Circular Cylinder," AIAA Journal, Vol. 6, No. 5, May 1968, pp. 815-822.

[3]Kitchens, Clarence W., Jr., "Numerical Experiments With the Compressible Navier-Stokes Equations," Proceedings of the Third International Conference on Numerical Methods in Fluid Mechanics, Vol. 1, Springer-Verlag, 1973.

[4]Payret, Roger and Viviand, Henri, "Calculation of the Flow of a Compressible Fluid Around an Obstacle of Parabolic Shape," TT F-16558, 1975, NASA.

[5]Grange, Jean-Marie, Klineberg, John M. and Lees, Lester, "Laminar Boundary Layer Separation and Near-Wake Flow for a Smooth Blunt Body at Supersonic and Hypersonic Speeds," AIAA Journal, Vol. 5, No. 6, June 1967, pp. 1089-1096.

[6]Weiss, R. F., "A New Theoretical Solution of the Laminar, Hypersonic Near Wake," AIAA Journal, Vol. 5, No. 12, December 1967, pp. 2142-2148.

[7]Reeves, Barry L. and Lees, Lester, "Theory of Laminar Near Wake of Blunt Bodies in Hypersonic Flow," AIAA Journal, Vol. 3, No. 11, November 1965, pp. 2061-2074.

[8]Weiss, R. F. and Weinbaum, S., "Hypersonic Boundary-Layer Separation and the Base Flow Problem," AIAA Journal, Vol. 4, No. 8, August 1966, pp. 1321-1330.

[9]Weinbaum, S., "Rapid Expansion of a Supersonic Boundary Layer and Its Application to the Near Wake," AIAA Journal, Vol. 4, No. 2, February 1966, pp. 217-226.

[10]Lykoudis, Paul S., "A Review of Hypersonic Wake Studies," AIAA Journal, Vol. 4, No. 4, April 1966, pp. 577-587.

[11]Crane, R. I., "A Survey of Hypersonic Near Wake Studies," The Aeronautical Journal of the Royal Aeronautical Society, Vol. 73, November 1969, pp. 998-1006.

[12]Berger, Stanley A., "Laminar Wakes," American Elsevier Publishing Company, Inc., New York, 1971.

[13]Allen, J. S. and Cheng, S. I., "Numerical Solutions of the Compressible Navier-Stokes Equations for the Laminar Near Wake," Phys. Fluids, Vol. 13, No. 1, January 1970, pp. 37-52.

[14]Ruger, Charles, "A Numerical Study of the Laminar Near-Wake of an Axisymmetric Body in a Supersonic Flow," General Applied Science Laboratories, Inc., Technical Report No. TR-763, October 1971.

[15]Gnoffo, Peter A., "A Generalized Orthogonal Coordinate System for Describing Families of Axisymmetric and Two-Dimensional Bodies," TM X-3468, 1977, NASA.

[16]Back, L. H., "Conservation Equations of a Viscous, Heat-Conducting Fluid in Curvilinear Orthogonal Coordinates," JPL Technical Report 32-1332, September 1968.

[17]Roache, Patrick J., "Computational Fluid Dynamics," Hermosa Publishers, Albuquerque, New Mexico, 1972.

[18]Allen, John S., Jr., "Numerical Solutions of the Compressible Navier-Stokes Equations for the Laminar Near Wake in Supersonic Flow," Ph.D Dissertation, Princeton University, June 1968.

[19]Barnwell, Richard W., "A Time-Dependent Method for Calculating Supersonic Angle of Attack Flow About Axisymmetric Blunt Bodies With Sharp Shoulders and Smooth Nonaxisymmetric Blunt Bodies," TN D-6283, August 1971, NASA.

[20]Van Dyke, Milton D., and Gordon, Helen D., "Supersonic Flow Past a Family of Blunt Axisymmetric Bodies," NASA Report 1, 1959.

[21]Moretti, G., "Circumspect Exploration of Multidimensional Imbedded Shocks," AIAA Journal, Vol. 14, No. 7, July 1976, pp. 894-899.

[22]Moretti, G., "Three-Dimensional, Supersonic, Steady Flows With any Number of Imbedded Shocks," AIAA Paper No. 74-10, January 1974.

[23]Salas, Manuel D., "Shock Fitting Method for Complicated Two-Dimensional Supersonic Flows," AIAA Journal, Vol. 14, No. 5, May 1976, pp. 583-588.

[24]Daywitt, J., Anderson, D. and Kutler, P., "Supersonic Flow About Circular Cones at Large Angles of Attack; A Floating Discontinuity Approach," AIAA Paper 77-86, January 1977.

[25]Tewfik, O. K. and Giedt, W. H., "Heat Transfer, Recovery Factor, and Pressure Distributions Around a Circular Cylinder Normal to a Supersonic Rarefied Air Stream," Journal of Aerospace Science, Vol. 27, No. 10, October 1960, pp. 721-729.

[26]Maslen, Stephen H., "On Heat Transfer in Slip Flow," Journal of the Aeronautical Science, June 1958, pp. 400-401.

[27]McCarthy, John F., Jr. and Kubota, Toshi, "A Study of Wakes Behind a Circular Cylinder at M = 5.7," AIAA Paper 63-170, June 1963.

[28]Graves, Randolph A., Jr., "Solutions to the Navier-Stokes Equations for Supersonic Flow Over Blunt Bodies With Massive Wall Blowing," Ph.D. Dissertation, George Washington University, November 1977.

[29]Hama, F. R., "Experimental Studies on the Lip Shock," AIAA Journal, Vol. 6, No. 2, February 1968, pp. 212-219.

[30]Erdos, J. and Zakkay, V., "Numerical Solution of Several Steady Wake Flows of the Mixed Supersonic/Subsonic Type by a Time-Dependent Method and Comparison With Experimental Data," AIAA Paper 69-649, June 1969.

Table 1 Calculated properties of Viking flowfields

M	Re	C_D	θ_{sep}, deg	L	$p_w(o)/p_\infty$	$T_w(o)/T_\infty$	p_{max}/p_∞
2	1,000	1.574	80.6	3.82	0.737	1.53	1.090
2	5,000	1.565	88.2	3.34	0.901	1.55	1.152
2	30,000	1.566	93.6	3.36	0.943	1.56	1.179
5	5,000	1.532	72.0	2.64	1.34	2.85	2.21
10	1,000	1.520	25.2	0.72	3.08	12.3	4.88
10	5,000	1.543	55.1	2.6	3.63	13.2	6.15

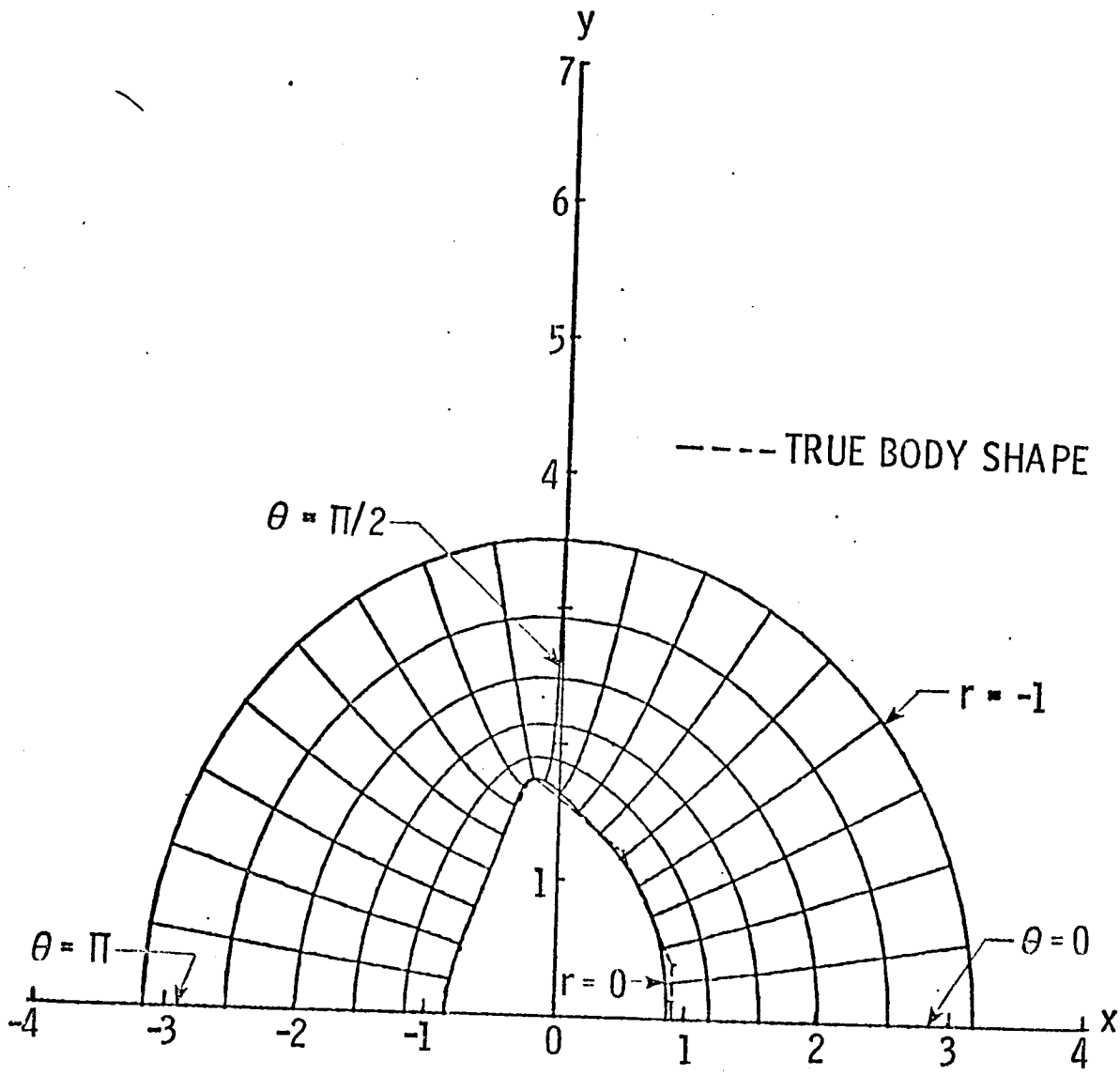

Fig. 1. Analytic approximation to Viking Aeroshell with associated coordinate lines.

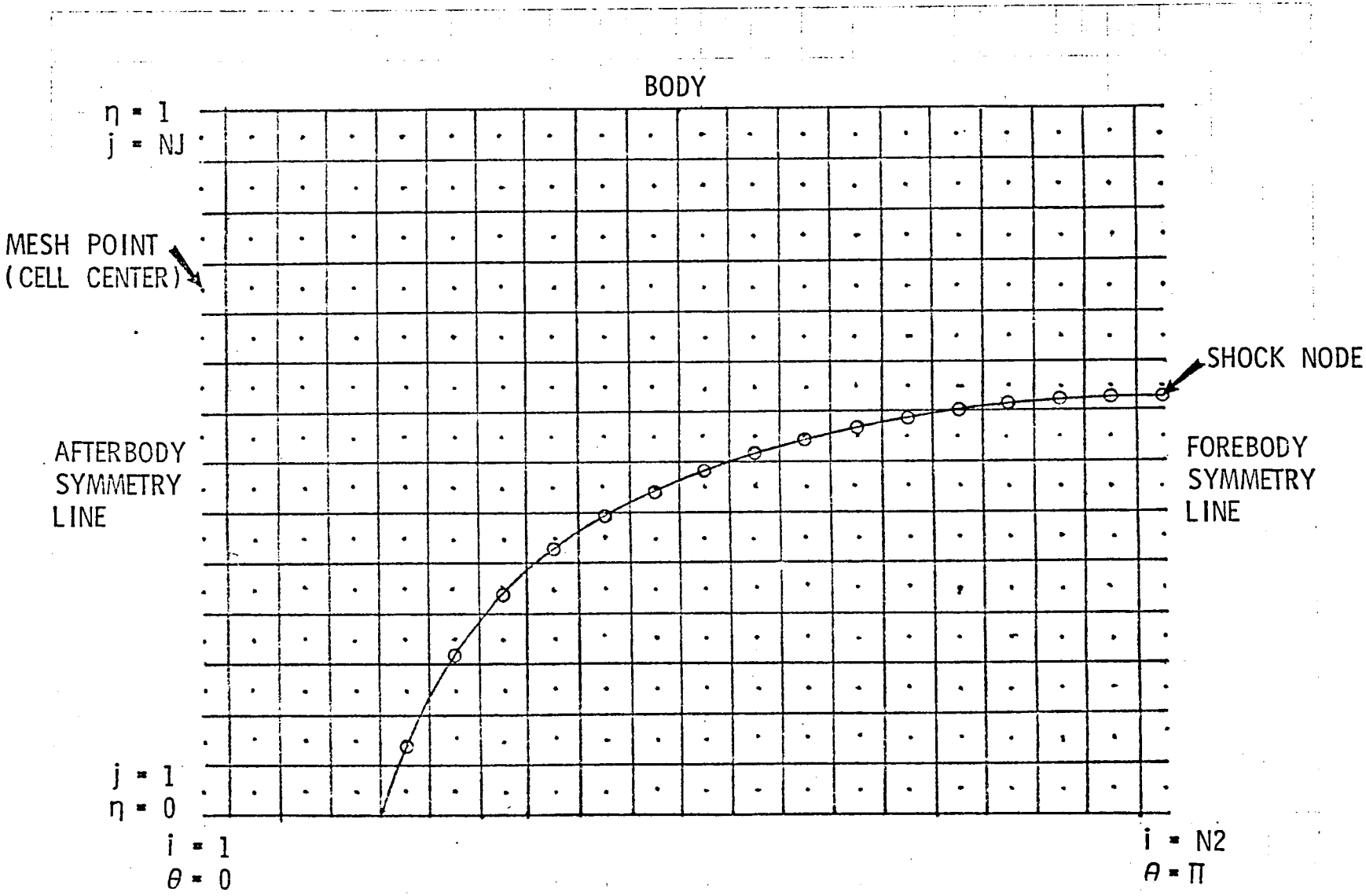

Fig. 2. Position of the floated shock in the computational plane.

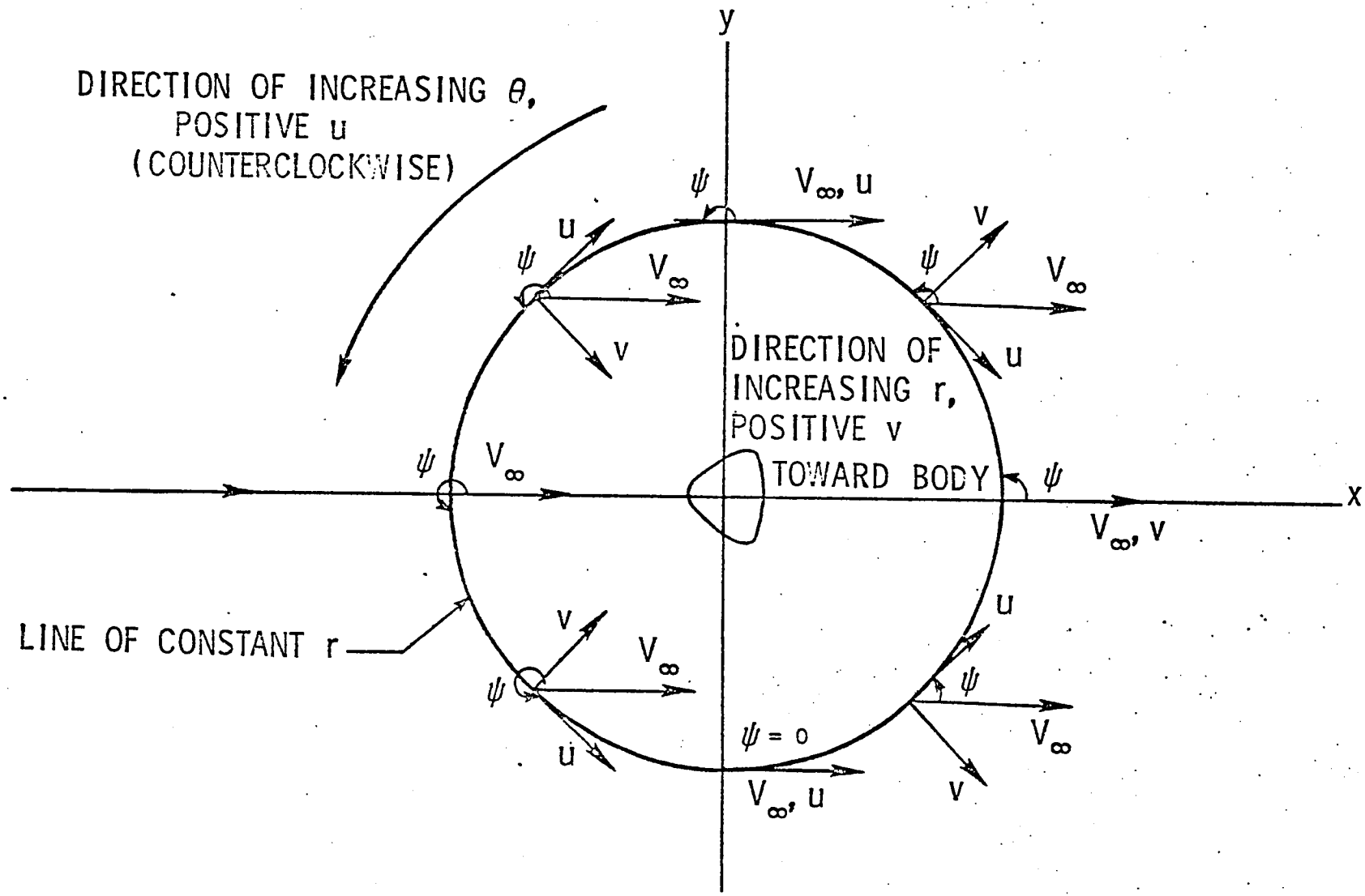

Fig. 3. Orientation of velocity vectors in transformed coordinate system.

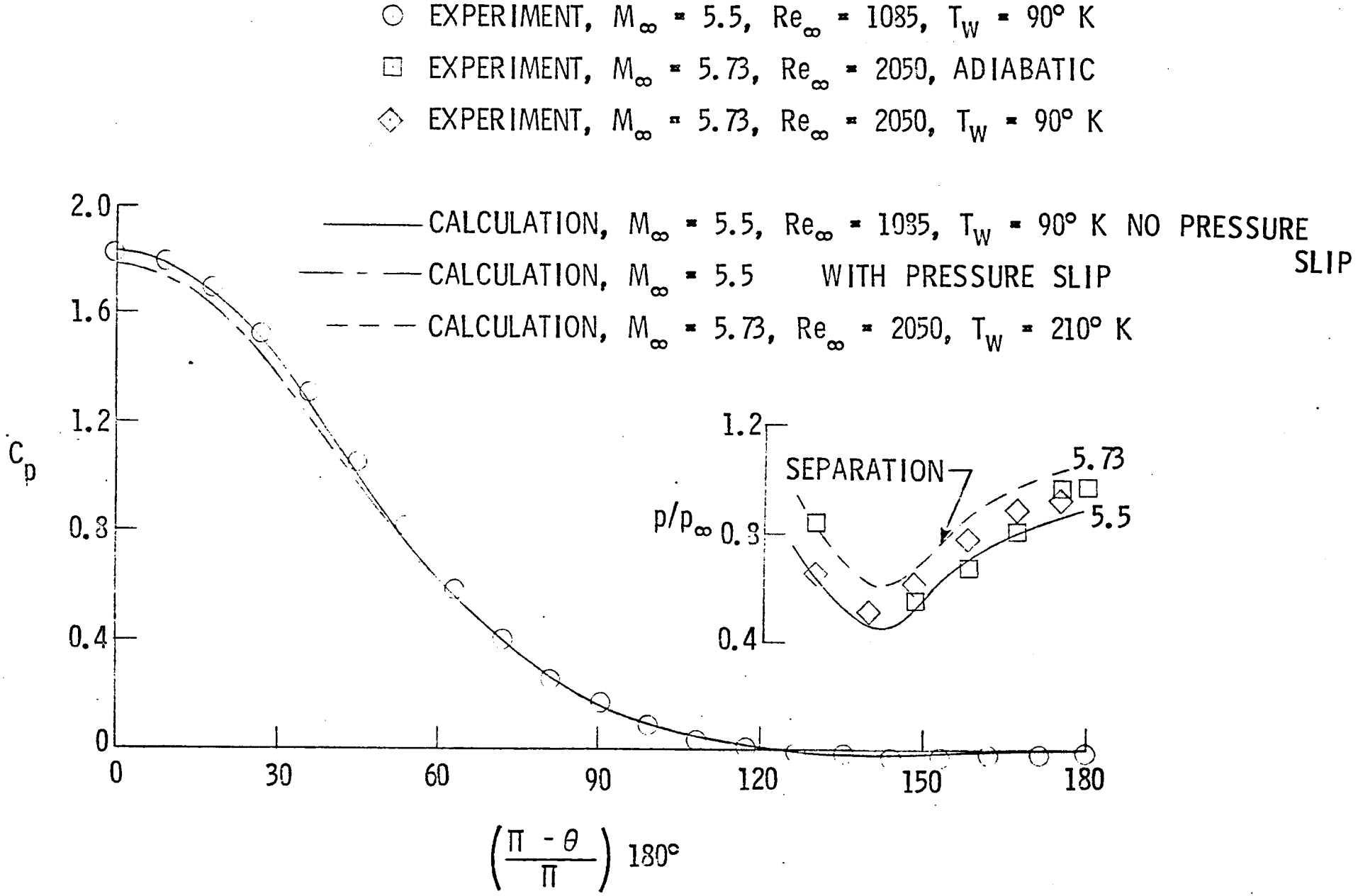

Fig. 4. Distribution of C_p and p/p_∞ over cylinder, T_0 = 300° K.

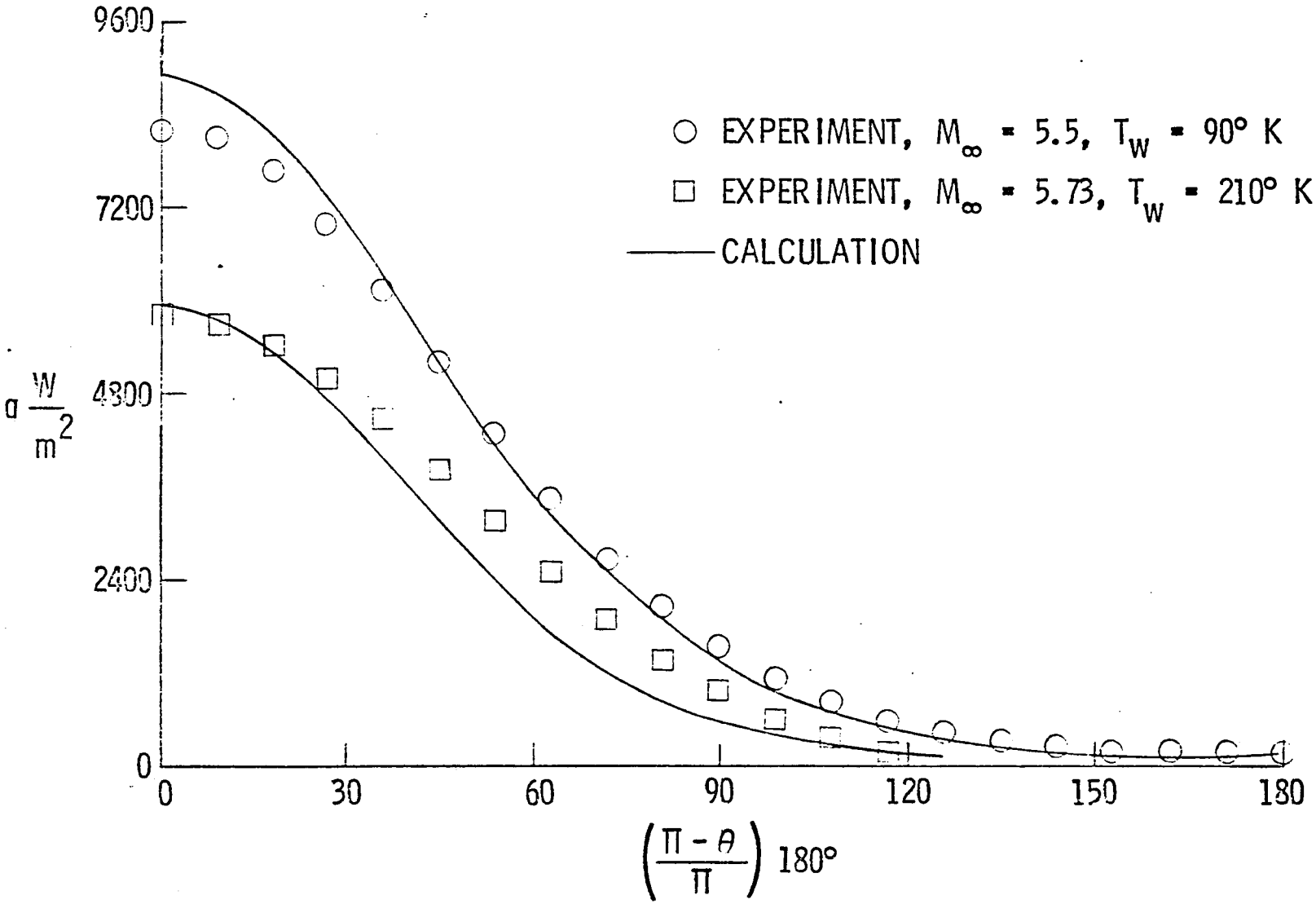

Fig. 5. Distribution of q over cylinder: $M = 5.5$, $Re = 1085$, $T_W/T_0 = 0.3$, $T_0 = 300°$ K
$M = 5.73$, $Re = 2050$, $T_W/T_0 = 0.68$, $T_0 = 300°$ K

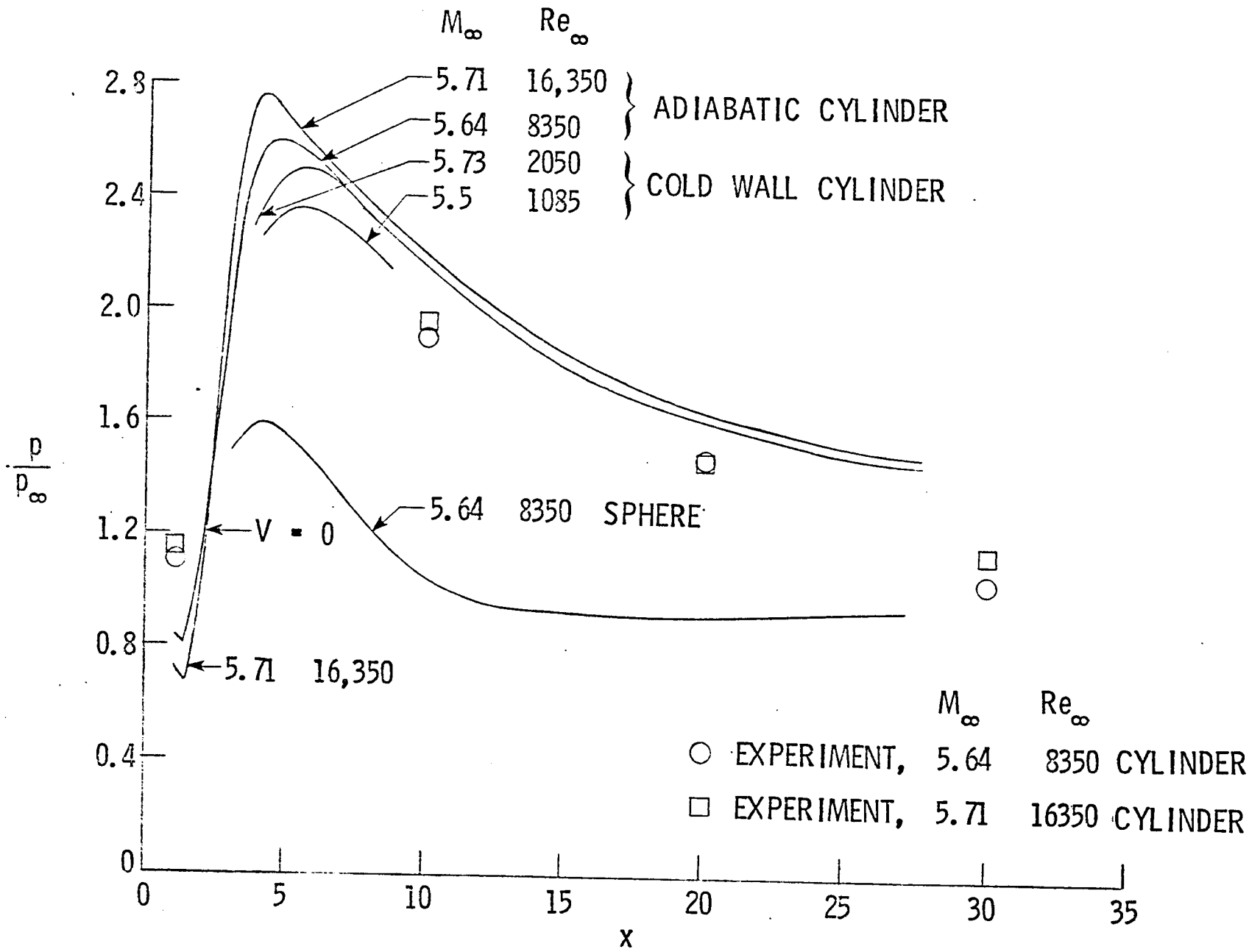

Fig. 6. Static pressure distribution on wake centerline.

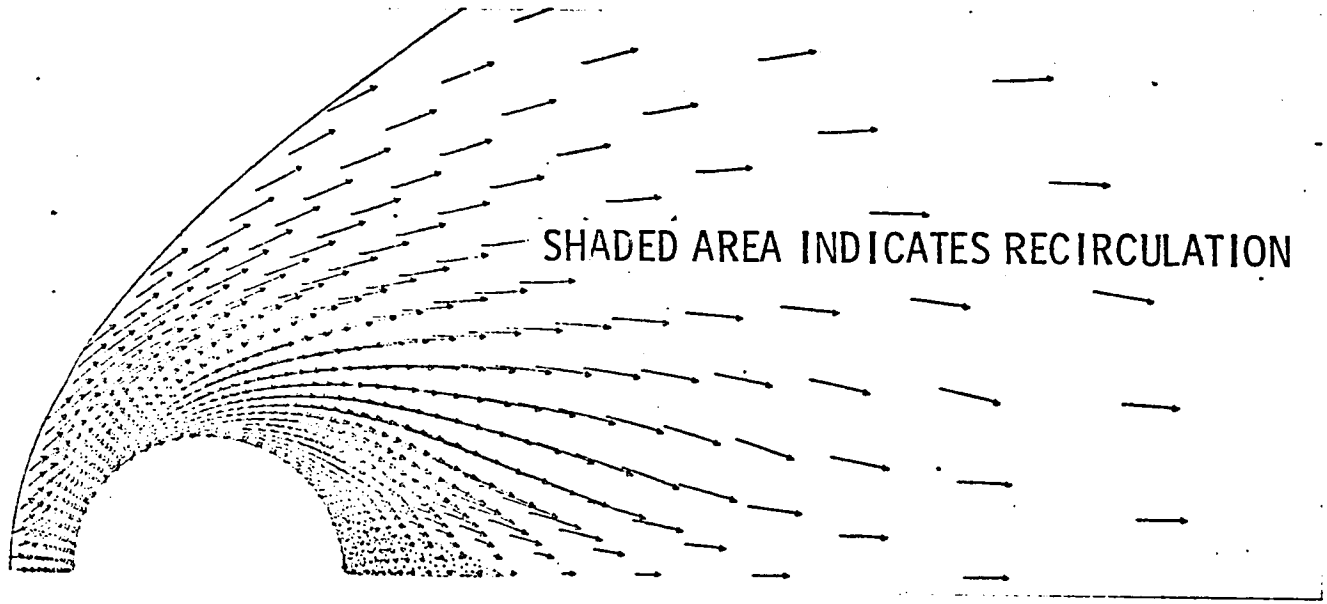

Fig. 7. Velocity vectors over cylinder, $M_\infty = 5.64$, $Re_\infty = 8350$.

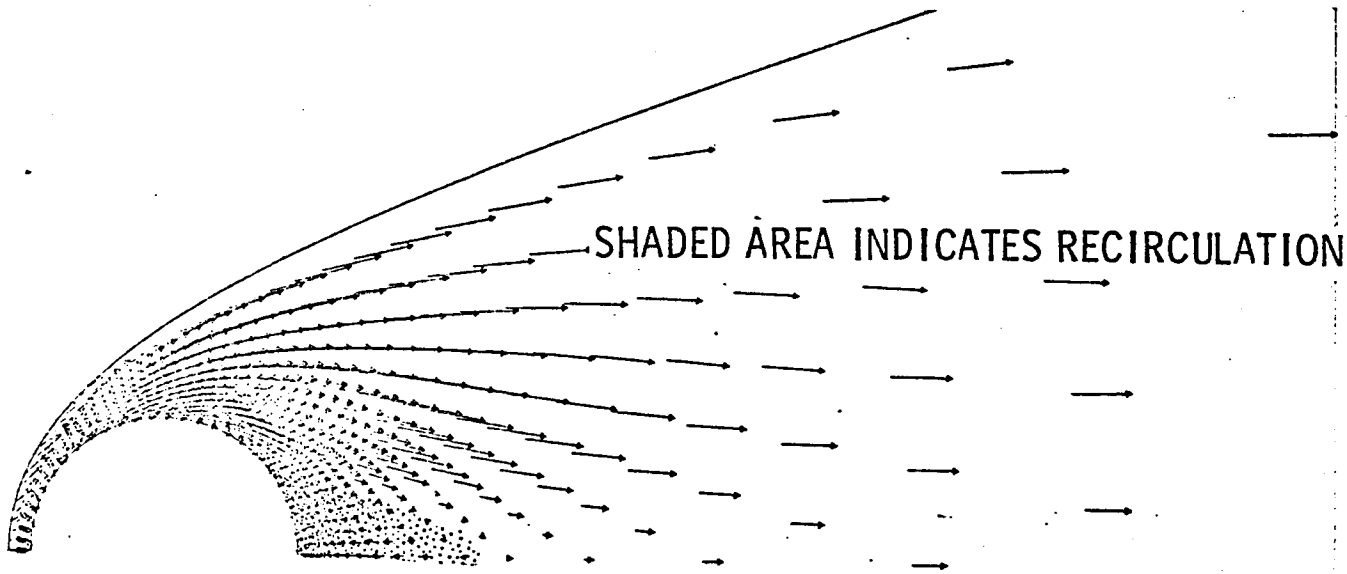

Fig. 8. Velocity vectors over sphere, $M_\infty = 5.64$, $Re_\infty = 8350$.

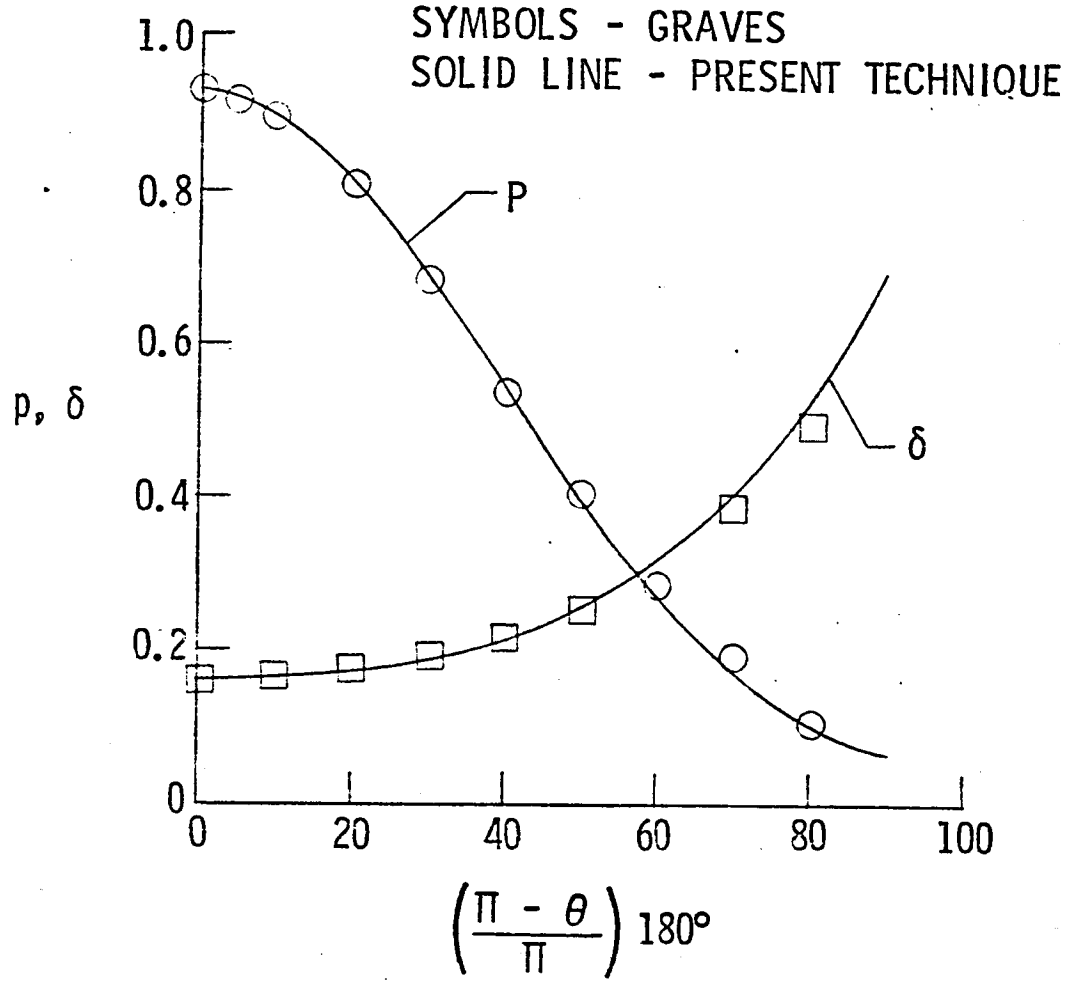

Fig. 9. Pressure and shock shape over sphere.

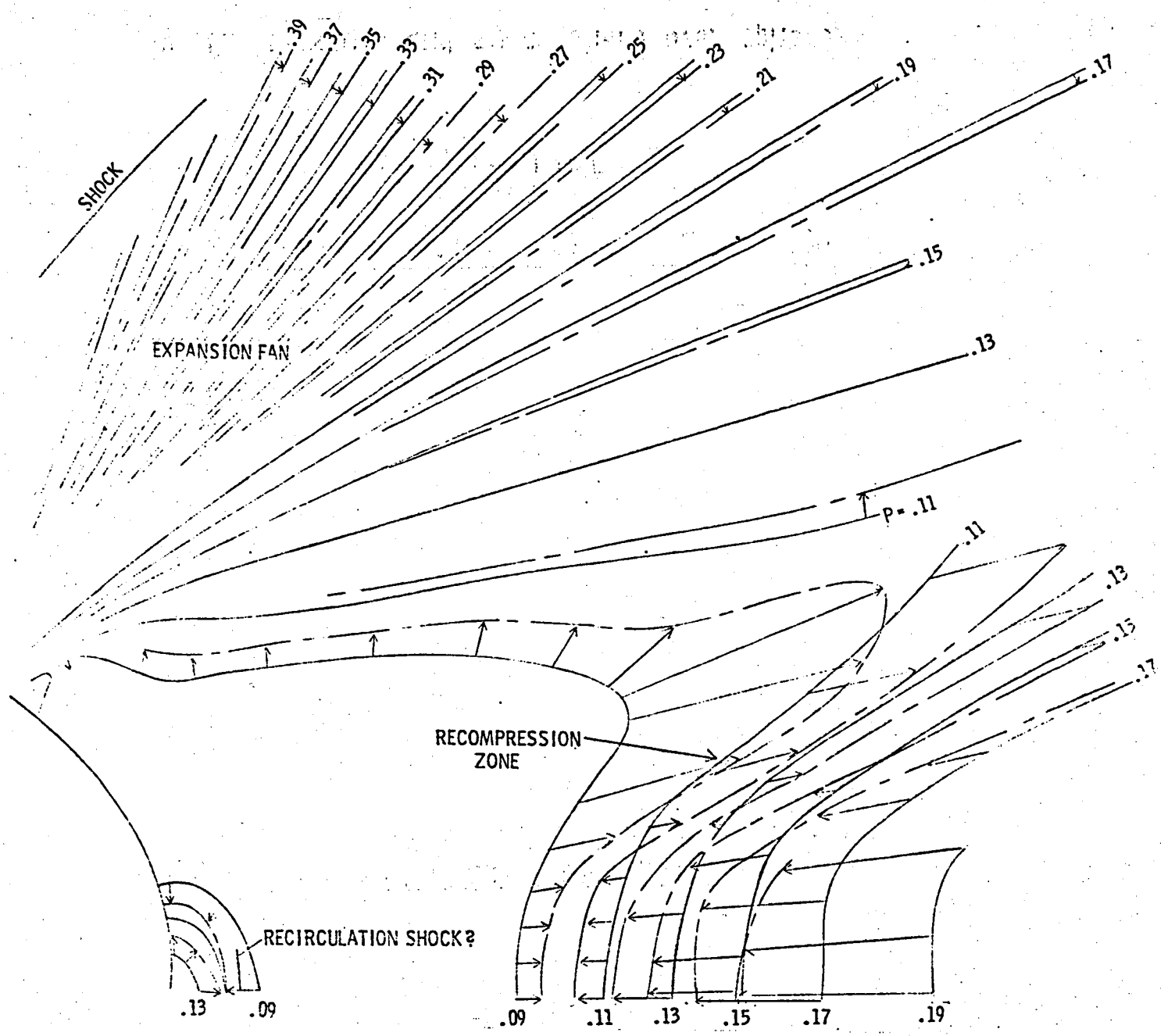

Fig. 10. Isobars over Viking Aeroshell for Re_∞ = 1000 and 30000.

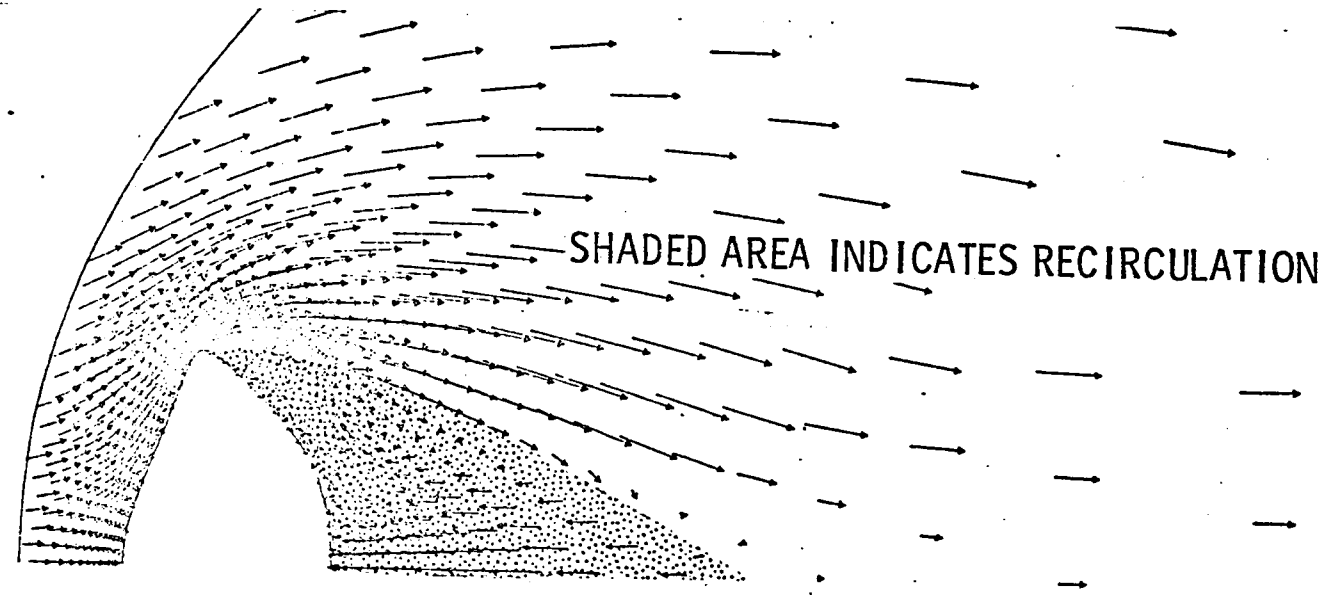

Fig. 11. Velocity vectors over Viking Aeroshell, $M_\infty = 2$, $Re_\infty = 5000$.

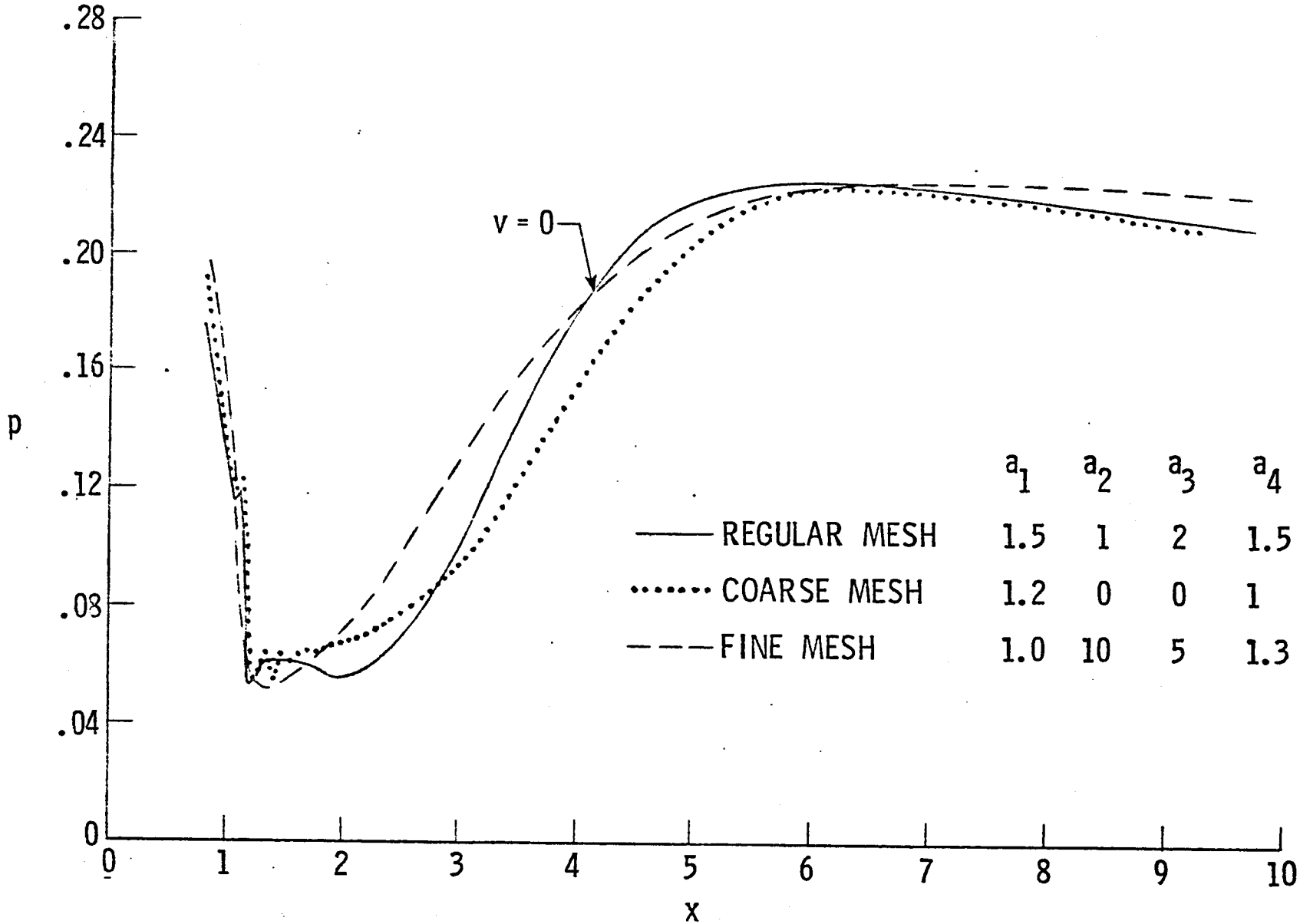

Fig. 12. Pressure distribution along wake symmetry axis for Viking Aeroshell, $M_\infty = 2$, $Re_\infty = 5000$.

1. Report No.	2. Government Accession No.	3. Recipient's Catalog No.
NASA TM-81784		

4. Title and Subtitle	5. Report Date
Complete Supersonic Flowfields Over Blunt Bodies in a Generalized Orthogonal Coordinate System	March 1980
	6. Performing Organization Code
7. Author(s)	8. Performing Organization Report No.
Peter A. Gnoffo	
9. Performing Organization Name and Address	10. Work Unit No.
NASA Langley Research Center Hampton, VA 23665	506-51-13-01
	11. Contract or Grant No.
	13. Type of Report and Period Covered
12. Sponsoring Agency Name and Address	Technical Memorandum
National Aeronautics and Space Administration Washington, DC 20546	14. Sponsoring Agency Code

15. Supplementary Notes

16. Abstract

A given orthogonal coordinate system is used to describe various axisymmetric and two-dimensional shapes. Close approximations to planetary probe configurations are possible. The full Navier-Stokes equations are discretized in this coordinate system in a manner based on Allen and Cheng's numerical procedure. The bow shock is treated as a discontinuity which floats between grid points. Completely coupled flows over the forebody, base, and near wake have been calculated over a cylinder, sphere, and an approximation to the Viking Aeroshell for $2 \leq M_\infty \leq 10$ and $1000 \leq Re \leq 30{,}000$. The program gives good comparisons with experimental data. A major contribution of this work is that it allows one to study the effect of changes in the blunt body shape on the base flow structure. Also, some problem areas in determining the base flow for increasing Reynolds number are discussed. In particular, it is found that the mean free path of the fluid near the wall immediately below the corner of the Viking Aeroshell, which experiences a severe expansion, can become greater than the local mesh size required to resolve the boundary layer in the forebody. Negative pressures, densities, and temperatures can be calculated in these instances. It appears that part of this problem is due to an inability to capture a lip shock close to the wall with the given grid.

17. Key Words (Suggested by Author(s))	18. Distribution Statement
Navier-Stokes equations Coordinate transformation Blunt body Wake flow Supersonic flow	Unclassified - Unlimited Subject Category: 34

19. Security Classif. (of this report)	20. Security Classif. (of this page)	21. No. of Pages	22. Price*
Unclassified	Unclassified	41	$4.50

For sale by the National Technical Information Service, Springfield, Virginia 22161